Study on magnetic properties for $La_{0.67}Sr_{0.33}MnO_{3-\delta}/Pr_{0.7}Ca_{0.3}MnO_{3-\delta}/La_{0.67}Sr_{0.33}MnO_{3-\delta}$ trilayer epitaxial film

2003 J. Phys.: Condens. Matter 15 7063

(http://iopscience.iop.org/0953-8984/15/41/014)

INSTITUTE OF PHYSICS PUBLISHING JOURNAL OF PHYSICS: CONDENSED MATTER

J. Phys.: Condens. Matter **15** (2003) 7063–7072 PII: S0953-8984(03)40150-1

Study on magnetic properties for $La_{0.67}Sr_{0.33}MnO_{3-\delta}/Pr_{0.7}Ca_{0.3}MnO_{3-\delta}/La_{0.67}Sr_{0.33}MnO_{3-\delta}$ trilayer epitaxial film

C S Xiong[1,2,5], Y H Xiong[1,3,4], G N Meng[2], Z P Jian[2], W Yi[2], Y T Mai[1], W Xu[1], S Yang[1], Z M Ren[1], J Zhang[1], X F Shi[1], Z C Xia[1] and S L Yuan[1]

[1] Department of Physics, Huazhong University of Science and Technology, Wuhan 430074, People's Republic of China
[2] Department of Physics, University of Science and Technology of China, Hefei 230026, People's Republic of China
[3] Department of Astronomy and Applied Physics, University of Science and Technology of China, Hefei 230026, People's Republic of China
[4] State Key Laboratory of Modern Acoustics, Nanjing University, Nanjing 210093, People's Republic of China

E-mail: csxiong@hust.edu.cn

Received 25 July 2002, in final form 21 July 2003
Published 3 October 2003
Online at stacks.iop.org/JPhysCM/15/7063

Abstract

We studied systematically the magnetic properties of $La_{0.67}Sr_{0.33}MnO_{3-\delta}/Pr_{0.7}Ca_{0.3}MnO_{3-\delta}/La_{0.67}Sr_{0.33}MnO_{3-\delta}$ trilayer epitaxial film fabricated on (001) $LaAlO_3$ single-crystal substrate using a direct current magnetron sputtering technique. A spin-glass-like behaviour and a magnetization relaxation phenomenon are observed from the results of the dependences of susceptibility on temperature (χ versus T curve) and magnetic relaxation on time (M versus t curve). The magnetic relaxation results are well fitted using the double-well-potential model. We also discussed the possible mechanism for the existence of spin-glass-like behaviour in the film. According to the χ versus T curves and the hysteresis loop, a magnetic anisotropy was observed in the film. The difference in electron-magnetic properties between $La_{0.67}Sr_{0.33}MnO_{3-\delta}$ single-layer epitaxial film and $La_{0.67}Sr_{0.33}MnO_{3-\delta}/Pr_{0.7}Ca_{0.3}MnO_{3-\delta}/La_{0.67}Sr_{0.33}MnO_{3-\delta}$ trilayer epitaxial film is also discussed.

(Some figures in this article are in colour only in the electronic version)

1. Introduction

Since the discovery of the colossal magnetoresistance (CMR) effect in manganese oxides, researchers have undertaken numerous works on the mechanism of the CMR effect [1–4].

[5] Author to whom any correspondence should be addressed.

There is growing interest in the heterostructures, trilayer and multilayer films combining ferromagnetic, superconducting, semiconductor, insulator and dielectric materials for their impact on both basic physical studies and the development of new electronic devices [5–15]. Because of the physical properties of spin glass, which raises many rather fundamental questions, there has been considerable interest in the spin-glass state of magnetic materials such as dilute magnetic alloys, amorphous materials and nanoparticle magnetic materials [16–18]. In recent years, some physicists have observed the phenomenon that spins are 'frozen' and aligned in random directions, and that the magnetic properties can be changed from a low spin moment distribution state to a high spin moment distribution state under some external conditions, such as the applied field and temperature in GMR (or CMR) materials, for example $La_{1-x}Ca_xMnO_3$, $La_{1-x}Ca_xMn_{1-y}Fe_yO_3$, $(TbLa)_{2/3}Ca_{1/3}MnO_3$ and $Eu_{0.58}Sr_{0.42}MnO_3$ perovskite manganites [19–23]. In particular, Rivadulla and López-Quintela [24] reported the magnetization and electron spin resonance (ESR) measurements around the Curie temperature on single-crystal and ceramic CMR manganites and considered inhomogeneities in similar materials. They also considered the dipole demagnetization field in these materials. Through these extensive works, it can be seen that the magnetic structure of this kind of materials plays a great role in their electronic transportation properties. Because magneto-electronic devices are potential candidates for magnetic random access memory, reading heads for tape and disk drives or magnetic field sensors [25], many efforts are being made to realize these applications using various magneto-transport devices.

Much research work has been performed based on trilayer or multilayer films, in which the materials of the middle layer include insulator, superconductor, dielectric, metal, semiconductor etc. We have studied the structure and magnetoresistance effect of trilayer $La_{0.67}Sr_{0.33}MnO_{3-\delta}/Pr_{0.7}Ca_{0.3}MnO_{3-\delta}/La_{0.67}Sr_{0.33}MnO_{3-\delta}$ (LPL for short) epitaxial films before [26]. Here we would like to discuss further the experimental results of the magnetic property measurements on the LPL trilayer film, such as the dependences of susceptibility on temperature and magnetic relaxation on time, as well as the hysteresis loop. Based on a thorough analysis of these experimental results, we conclude that there exists a spin-glass-like behaviour, which is probably caused by the competition between ferromagnetism and antiferromagnetism in the trilayer epitaxial film. After fitting the parameters of the relaxation experiment according to the double-well-potential model, we also obtain some dynamical properties of the sample. A comparison of electron-magnetic properties between $La_{0.67}Sr_{0.33}MnO_{3-\delta}$ (LSMO for short) single-layer epitaxial film and LPL trilayer epitaxial film is also discussed.

2. Experimental details

The trilayer epitaxial films were fabricated using a direct current magnetron sputtering method, which has been discussed in detail in a previous paper [26]. A thin-film sample was made up of three layers, with the upper and bottom layers both being $La_{0.67}Sr_{0.33}MnO_{3-\delta}$ of the same 150 nm thickness and the middle layer being $Pr_{0.7}Ca_{0.3}MnO_{3-\delta}$ (PCMO) of 30 nm thickness. The film was sputtered onto a $LaAlO_3$ single-crystal substrate of (001) orientation at a temperature (T_S) of 600 °C. After deposition, the sputter chamber was immediately filled with 7 SCCM O_2 only and the gas pressure was kept to 4 Pa, under which the film was cooled down to room temperature. The surface morphology of the film was obtained using scanning tunnelling microscopy (STM).

The magnetic properties were measured using a commercial superconducting quantum interface device (SQUID) magnetometer with the temperature ranging from 4.2 to 300 K and the applied magnetic field ranging from 0.01 to 1.00 T (Tesla). The temperature dependence of

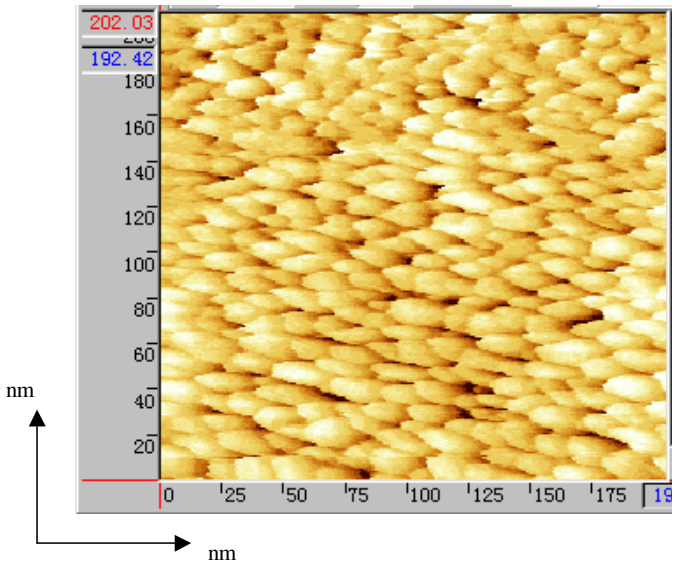

Figure 1. The surface morphology of an LPL trilayer film obtained by STM.

the sample's susceptibility (χ) was, respectively, measured under zero field cooling (ZFC) and field cooling (FC) from room temperature under a certain applied field, which is a standard experimental approach to the system of metamagnetism. The results of the dependence of magnetic relaxation on time were obtained at several different temperatures (ranging from 4.2 to 300 K) and under an applied magnetic field of 0.1 T. The measurement of the magnetic hysteresis loop was conducted under three different temperatures (10, 50 and 100 K) with the applied field perpendicular to the film plane and parallel to the film plane, respectively.

2.1. Results and discussions

The surface morphology of the LPL trilayer film obtained by STM is shown in figure 1. From this it can be observed that the surface consists of many three-dimensional columns, which are uniform granular structures with a size of 20 nm. This result confirms the x-ray diffraction results, in which our films are measured to be high-quality epitaxial films [27].

Figure 2 shows the curve of the external applied field (H) versus the freezing temperature (T_f), in which the solid symbols stand for experimental data and the line denotes the fitting curve. The inset in figure 2 is the temperature dependence of susceptibility (χ) for the LPL trilayer film and the LSMO single-layer film. From the inset of figure 2, we can observe that there are two magnetic transitions in the trilayer film sample at two different temperatures: the Curie temperature (T_C) and T_f, which is a similar phenomenon to that observed in an LSMO single-layer film sample [28]. T_C is a constant temperature of about 260 K. This is reasonable since T_C is principally determined by the sample's structure, and the structure does not change for different values of H. But T_f becomes smaller with increasing H, which indicates a transition from metamagnetism to ferromagnetism. The cusps appearing on the ZFC curves are a typical characteristic of a spin-glass system. We can attribute the origin of the spin-glass-like behaviour in epitaxial film system to the disordered distribution of Mn^{3+} and Mn^{4+} ions and the competition between ferromagnetic and antiferromagnetic interactions, as we have previously interpreted the spin-glass-like behaviour in LSMO single-layer film [28]. By using

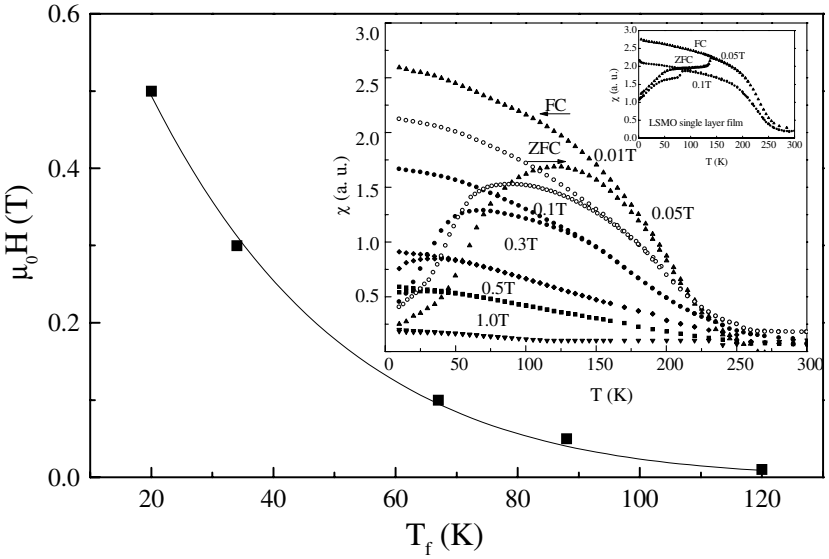

Figure 2. The curve of H versus T_f. The inset is the temperature dependence of the susceptibility for an LPL trilayer film and a LSMO single-layer film.

the energy provided by the external applied field, the directions of spin clusters in the spin-glass state can change from a random distribution state to the direction of the applied field, thus the system will need less thermal energy to defrost from the spin-glass state. Therefore, the freezing temperature will shift into a lower temperature range with an increase in the external field.

Also from the inset of figure 2, we can observe the difference in magnetic properties (such as the shape of the χ–T curves and the values of T_f) between an LSMO single-layer film and an LPL trilayer film. It is necessary to point out the different definition of the freezing temperature (T_f) for a single-layer LSMO film and an LPL trilayer film. In the usual spin-glass terminology, T_f is the temperature of the starting point of magnetic irreversibility, which for most samples is the temperature, where there is a maximum of susceptibility. We did the same as this before [28]. But in LPL trilayer films, there is an unusual relation between susceptibility and temperature, where there is no maximum of susceptibility in the temperature, which is the starting point of magnetic irreversibility. So for LPL trilayer films, we choose the temperature at which there is a maximum of susceptibility as T_f. In other words, we compare the LSMO single-layer film and the LPL trilayer film at the temperature at which there is the maximum.

In figure 2, the experimental data can be fitted quantitatively very well by the equation

$$H = H_0\left(1 - \frac{T_f}{T_C}\right)^b \tag{1}$$

where H_0 is a critical field above which T_f is zero, b is a scale parameter, and T_C is the Curie temperature. Using equation (1), we can calculate two parameters, H_0 and b, which are $\mu_0 H_0 = 0.911$ T and $b = 8.26$, respectively. From figure 2, it is obvious that there is a well matched relation between H and T_f.

It is interesting to see what the effect of the middle PCMO layer is by comparing the electronic and magnetic properties of the LPL trilayer film with those of the LSMO single-layer film. The addition of the middle PCMO layer results in an increase in the metal–insulator

Table 1. The parameters of the LSMO single-layer film and the LPL trilayer film.

	$La_{0.67}Sr_{0.33}MnO_{3-\delta}$ film				$La_{0.67}Sr_{0.33}MnO_{3-\delta}/Pr_{0.7}Ca_{0.3}MnO_{3-\delta}/La_{0.67}Sr_{0.33}MnO_{3-\delta}$ film			
Thickness (nm)	600				150/30/150			
T_P (K)	173				175			
ρ_{max} (10^{-3} Ω cm)	17.11				7.770			
E_c (eV)	0.158				0.137			
$\mu_0 H$ (T)	0.05	0.08	0.10	0.30	0.05	0.10	0.30	0.50
T_f (K)	140	122	90	41	88	67	34	20
χ (10^{-7} au)	2.24	1.91	1.87	1.49	1.54	1.29	0.85	0.54

transition temperature (T_p) and a decrease in the peak resistivity (ρ_{max}), hence the middle PCMO layer has the same effect as the external applied field [26]. Table 1 lists the parameters of the LSMO single-layer and LPL trilayer films. From this, we can see that the electronic and magnetic properties of the LPL trilayer film are similar to those of the LSMO single-layer film, except for some minor differences in the values of parameters. T_f of the LPL trilayer film is lower than that of the LSMO single-layer film under the same applied field. According to the effect of the applied field on the freezing temperature (see the inset of figure 2, in which T_f decreases with an increase of applied field), it is possible to conclude that the middle PCMO layer also results in a shift of the freezing temperature for the LPL trilayer film and it seems that there already exists an internal magnetic field to help the system to defrost from the spin-glass state into the ferromagnetic state. We cannot draw any conclusion about the exact values of susceptibility in our measurement, since the samples were broken up into small unequal pieces with an area of about 4 mm^2 when the measurements were made. So, we could not measure the mass of our thin-film sample and the susceptibility does depend on the total mass (or volume) of the whole sample. At the same time, in the lower-temperature vicinity of T_f, the slopes of LPL's cusps, where the metamagnetism occurs, are smoother than those of LSMO. So, the effect of PCMO on the magnetization is an interesting topic. From the experimental phenomenon above, we can see that there is an intra-magnetic coupling within LPL trilayer films, and that the magnetic coupling may result in the formation of more magnetic clusters in the film. These extra spontaneous clusters will make the transition from metamagnetsim to ferromagnetism easier by competing with the external applied field in rotating magnetic clusters, so the magnetization curve for LPL looks smoother than that for LSMO in the vicinity of the metamagnetism transition. By comparing the metamagnetism behaviour of the LPL trilayer and LSMO single-layer films, we come to the same conclusion that the addition of middle PCMO layer has a similar effect on the external applied magnetic field. Also, the difference in the parameters $\mu_0 H_0$ and b calculated using equation (1) ($\mu_0 H_0 = 0.911$ T and $b = 8.26$ for the LPL trilayer film and $\mu_0 H_0 = 0.574$ T and $b = 3.929$ for the LSMO film) can be explained by the additive effect of the middle PCMO layer.

Figure 3 shows the relaxation behaviour of magnetization (M) with an external applied field of $\mu_0 H_0 = 0.1$ T, for temperatures $T = 30$, 50, 70, 100 and 150 K, respectively. It shows another typical property of a spin-glass system that there is a long relaxation time, which represents the irreversible magnetization process of the spin-glass system. Figure 3 also presents the fact that there is a meta-stable magnetic characteristic in our film sample. Through studying the results of magnetization relaxation, we can obtain information about the dynamic properties of the magnetic clusters. Here we use the double-potential-well model to derive the relaxation relations of the LPL trilayer film, just as we did for the LSMO single-layer film [28]. Due to the antiferromagnetic interactions between ions, antiferromagnetic clusters are formed

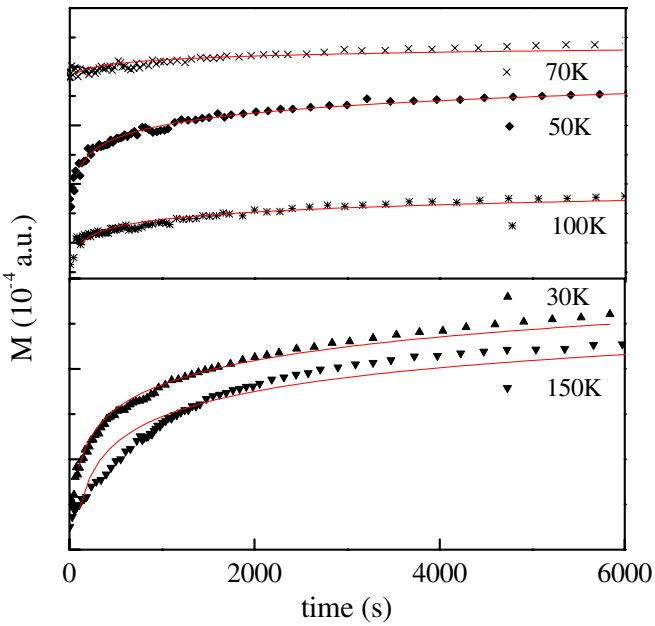

Figure 3. The relaxation relation between M and time ($\mu_0 H = 0.1$ T).

below the Curie temperature and, because of the random distribution of Mn^{3+} and Mn^{4+} ions, magnetic moments are organized into ferromagnetic clusters with different sizes and directions. Thus we can reasonably focus our attention on the contribution of ferromagnetic clusters to the magnetization process of the spin-glass system.

According to the double-well-potential model, the relationship between magnetization and time obeys the following equation:

$$M = \alpha - \beta\left(\frac{t}{t_0}\right)^{-\gamma} \tag{2}$$

where α and β are the time-independent parameters for varied temperatures. γ is larger than zero and is a time-independent parameter, but it is dependent on temperature. t_0 is the time when the measurement begins.

Considering the limit $t \to \infty$ and $t = t_0$ respectively, we can see that α represents the value of M of the final equilibrium state and α–β represents the initial magnetic state of the sample. With increasing time, the spin system of the sample will gradually change its state from α–β to α, or change from one kind of spin distribution state to a more stable kind under the influence of the applied field.

The experimental data in figure 3 can be fitted well using equation (2), except for where the temperature is 150 K. The temperature 150 K is higher than the freezing temperature and, at this temperature, the system has passed the transition from metamagnetism to ferromagnetism. The open circles and solid squares in figure 4 represent the experimental data and calculated data, respectively. We obtain the values of α, β and γ for separate temperatures and can conclude that the values of γ and α–β increase as temperature rises, while α decreases. According to the double-well-potential theory, the physical meaning of the parameter γ is related to the excitation energy, so we can obtain information about the dynamical properties of the excitation energy.

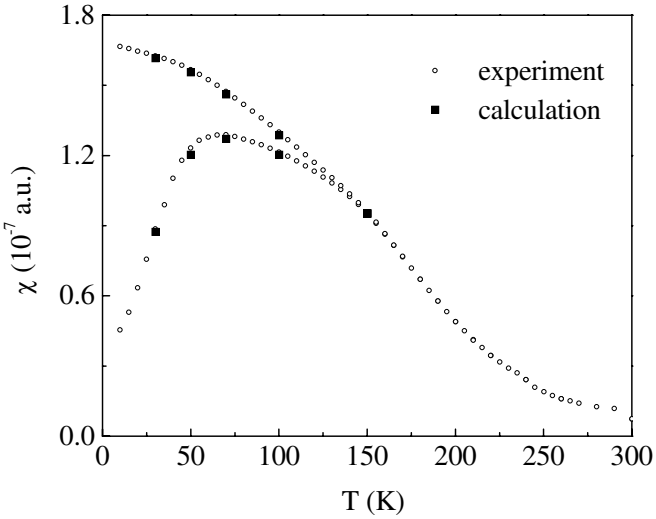

Figure 4. The comparison between the experimental data and the calculated data ($\mu_0 H = 0.1$ T).

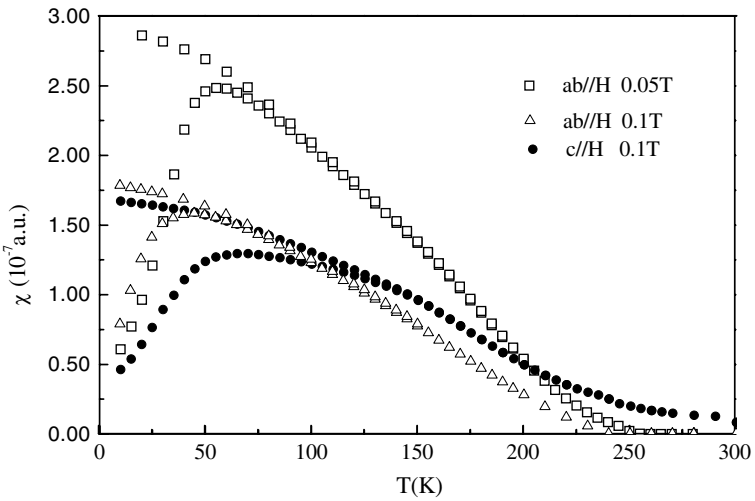

Figure 5. The relation between χ and T for different applied fields and directions.

Figure 5 shows the relationship between χ and T in different applied fields. We took the measurement for the LPL trilayer film with $\mu_0 H_0 = 0.05$ and 0.1 T, and the direction of the applied field is perpendicular to the film (denoted $c \parallel H$) and parallel to the film (denoted $ab \parallel H$), respectively. From figure 5, we can see that the freezing temperature for $c \parallel H$ is obviously higher than the freezing temperature for $ab \parallel H$. This indicates the magnetic anisotropy inherent in the film.

Figure 6 shows the relationship between the magnetization M and H when $T = 10$ K, and the insets show the relationship between the magnetization M and H when $T = 50$ and 100 K, respectively. In figure 6, we can see that there is a usual hysteresis. Also, the higher the saturation magnetization, the lower the temperature. We can also see that the

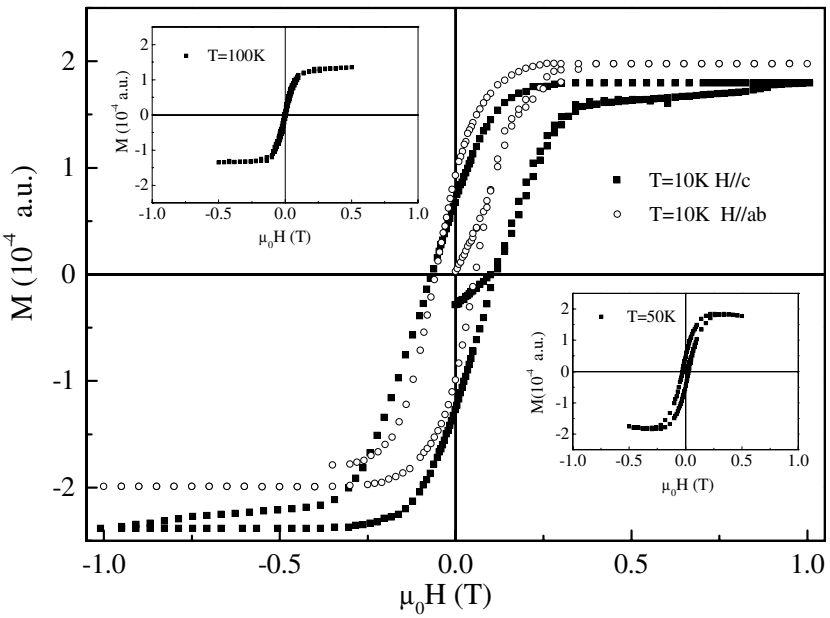

Figure 6. The relation between M and H for $T = 10$, 50 and 100 K (and for different directions of the applied field).

Table 2. The anisotropy parameters of the LPL trilayer film.

	$La_{0.67}Sr_{0.33}MnO_{3-\delta}/Pr_{0.7}Ca_{0.3}MnO_{3-\delta}/La_{0.67}Sr_{0.33}MnO_{3-\delta}$ film	
	$H \parallel c$	$H \parallel ab$
M_s (10^{-4} au)	1.32 ($T = 100$ K) 1.82 ($T = 50$ K)	
	1.97 ($T = 10$ K)	1.99 ($T = 10$ K)
M_r (10^{-4} au)	0.12 ($T = 100$ K) 0.47 ($T = 50$ K)	
	0.92 ($T = 10$ K)	0.93 ($T = 10$ K)
$\mu_0 H_c$ (T)	0.01 ($T = 100$ K) 0.03 ($T = 50$ K)	
	0.10 ($T = 10$ K)	0.06 ($T = 10$ K)
χ_0 (10^{-7} au)	0.43 (0.05 T)	0.61 (0.05 T)
	0.45 (0.1 T)	0.79 (0.1 T)
χ_{max} (10^{-7} au)	2.12 (0.05 T)	2.86 (0.05 T)
	1.67 (0.1 T)	1.79 (0.1 T)
T_f (K)	88 (0.05 T)	55 (0.05 T)
	67 (0.1 T)	43 (0.1 T)

hysteresis loop changes when the direction of applied field is changed. Table 2 shows the anisotropy parameters of the LPL trilayer film, from which we can again see the anisotropy properties of the magnetization. Many factors could result in the anisotropy property, but here we suggest two possible mechanisms: one is the substrate orientation. Different substrate orientations result in different film orientations, and the magnetic properties of films with different orientations—including the freezing temperature, susceptibility or magnetization, hysteresis loop etc—are different. The difference in the magnetic properties will influence the electron-transport behaviour, including T_P and ρ_{max}. This opinion has been substantiated further by systematically studying the effect of oxygen partial pressure on the electro-magnetic

properties for $La_{0.67}Sr_{0.33}MnO_{3-\delta}$ epitaxial films with different orientations [29]. The other possible mechanism is the effect of the dipole demagnetization field with this thin-film geometry. Further research on this topic is expected to yield a through understanding.

3. Conclusions

With thorough investigation of the magnetic properties of LPL trilayer epitaxial film, we can observe spin-glass-like behaviour in our present sample as well as the anisotropy properties of the magnetization. The competition of two different magnetic interactions in the sample results in the formation of the magnetic moment clusters, which play an important role in the temperature dependence of magnetization, magnetic relaxation and the hysteresis loop. The double-well-potential model was used to fit our relaxation experimental data, in order to study in detail the energy spectroscopy information. By comparing the result for the LPL trilayer film with that for the LSMO single-layer film, we can conclude that the middle PCMO layer does act equivalently to an external field. It is this effect that causes the differences in electro-magnetic properties between LSMO and LPL trilayer films. To explain the anisotropy properties of LPL trilayer film, two mechanisms are suggested: one is the different orientation of the films and the other is the effect of the dipole demagnetization field. It would be more interesting to compare the spin-glass property and structures of these trilayer films further after convenient optimized annealing processes at different temperatures. This would also aid the understanding of whether spin-glass properties are localized or not in trilayer films and provide extended experimental evidence.

Acknowledgments

The authors would like to thank Professor X G Li, Dr L Pi, D G Zong, J F Zhang and Y F Deng. This work was supported by the National Science Foundation of China (grant no 10274022) and the School of Science Foundation of the Huazhong University of Science and Technology.

References

[1] von Helmolt R, Wecker J, Holzapfel B, Schultz L and Samwer K 1993 *Phys. Rev. Lett.* **71** 2331
[2] Jin S, Tiefel T H, McCormack M, Fastnachr P A, Ramesh R and Chen L H 1994 *Science* **264** 413
[3] Xiong G C, Li Q, Ju H K, Mao S N, Senapati L, Xik X X, Greene R L and Venkatesan T 1995 *Appl. Phys. Lett.* **66** 1427
[4] Ziese M 2002 *Rep. Prog. Phys.* **65** 143
[5] Chahara K *et al* 1993 *Appl. Phys. Lett.* **62** 780
[6] Yin H Q, Zhou J S and Goodenough J B 2000 *Appl. Phys. Lett.* **77** 714
[7] Hwang H Y, Cheong S-W and Batlogg B 1996 *Appl. Phys. Lett.* **68** 3494
[8] Sun J Z, Gallagher W J, Duncombe P R, Krusin-Elbaum L, Altman R A, Gupta A, Lu Y, Gong G Q and Xiao G 1996 *Appl. Phys. Lett.* **69** 3266
[9] Sun J Z 2001 *Physica* C **350** 215
[10] Cheng R S, Li K B, Wang S G, Chen Z X, Xiong C S, Xu X J and Zhang Y H 1998 *Appl. Phys. Lett.* **72** 2475
[11] Chakalov R A, Mikheenko P, Severac C H L, Allsworth M, Darlington C N W, Wellhőfer F and Muirhead C M 2000 *Physica* C **341–348** 2725
[12] Isa M, Nishizaki T, Fujiwara M, Naito T and Kobayashi N 1997 *Physica* C **282–287** 691
[13] Kwon C, Jia Q X, Fan Y, Hundley M F, Reagor D W, Coulter J Y and Peterson D E 1998 *Appl. Phys. Lett.* **72** 486
[14] Tanaka H, Okawa N and Kawai T 1999 *Solid State Commun.* **110** 191
[15] Sarkar S, Raychaudhuri P, Nigam A K and Pinto R 2001 *Solid State Commun.* **117** 609
[16] Uhlmann D R 1978 *Metallic Glasses* (Metals Park, OH: American Society for Metals) chapter 6
[17] Guo Y C and Wang Z X 1984 *Non-Crystalline Physics* (Beijing: Science Publisher) chapter 3 (in Chinese)

[18] Mydosh J A 1993 *Spin Glasses: an Experimental Introduction* (London: Taylor and Francis)
[19] Von Helmolt R, Wecker J, Lorenz T and Samwer K 1995 *Appl. Phys. Lett.* **67** 2093
[20] Zhang X X, Yu R H, Tejada J, Sun G F, Xin Y and Wong K W 1996 *Appl. Phys. Lett.* **68** 3191
[21] Cai J W, Wang C, Shen B G, Zhao J G and Zhan W S 1996 *Appl. Phys. Lett.* **71** 1727
[22] De Teresa J M *et al* 1996 *Phys. Rev. Lett.* **76** 3392
[23] Sundaresan A, Maignan A and Raaveau B 1997 *Phys. Rev.* B **55** 5596
[24] Rivadulla F and López-Quintela M A 1999 *Phys. Rev.* B **60** 11922
[25] Prinz G A 1998 *Science* **282** 1660
[26] Xiong C S, Tang Y Q, Gao J, Zhu H, Pi L, Li K B, Zhu J S and Zhang Y H 1999 *Phys. Rev.* B **59** 9437
[27] Xiong C S, Pi L, Xiong Y H, Jia Y B, Zhou G E, Jian Z P and Li X G 2000 *Solid State Commun.* **114** 341
Xiong C S, Xiong Y H, Jia Y B, Jian Z P, Zhou G E, Pi L, Mai Y T, Xia Z C and Yuan S L 2003 *Mater. Res. Bull.* **38** 1183
Gao J, Xiong C S, Tang Y Q, Zhu H, Pi L, Zhu J S, Zhou G E and Zhang Y H 1997 *Chin. Sci. Bull.* **42** 1932
[28] Xiong C S, Xiong Y H, Yi W, Meng G N, Xia Z C, Li X G and Yuan S L 2002 *J. Phys.: Condens. Matter* **14** 4309
[29] Xiong C S, Luo Z L, Xiong Y H, Meng G N, Jian Z P, Yi W, Zong D G, Xia Z C and Yuan S L 2003 *J. Magn. Magn. Mater.* **257** 369